Microcontroller-based lock-in amplifier: A comparative study

Diogo Rikio Miyazaki
diogo.miyazaki@gmail.com

Dr. Marlio J. C. Bonfim
marlio.b@eletrica.ufpr.br

Dr. Eduardo Parente Ribeiro
edu@eletrica.ufpr.br

M.Sc. Rafael da Silva Ferraz
rafael.silvaferraz@gmail.com

Raiff S. da Fonseca
raiffsf@gmail.com

Department of Electrical Engineering
Federal University of Parana, Curitiba, Brazil

***Abstract* — This paper presents a new approach to the classical design and implementation of a Lock-In Amplifier (LIA) applied to impedance measurement of resistances, capacitances, inductors and their arrangements. It is based on a general-purpose microcontroller and an active band-pass filter. The design uses a low frequency Pulse Width Modulation (PWM) as source for the reference signal and an Analog to Digital Converter (ADC) from the microcontroller to sample the device under test (DUT) signal. In the particular context of this study, the results are limited to discrete components with relative error around 10%, which rises with higher impedance magnitudes. The measurement error pattern observed in RC, RL and LCR is also presented in this paper in order to emulate practical applications.**

Keywords* — *Lock-in amplifier, microcontroller, impedance, phase sensitive detection.

I. INTRODUCTION

LIA is an instrumentation technique used in laboratories for a wide variety of purposes [1-3], due to its capability of measuring a single frequency signal obscured by noise. It is based on a phase sensitive detector (PSD) and must be set to operate at a desired frequency.

The design of a classical LIA is presented in Fig. 1. Two signals, one reference and one input, are multiplied in phase and in quadrature by the PSD. Each resulting signal is then filtered by a narrow lowpass filter, whose main purpose is to filter out the high frequency component resulting from the multiplication, as well as the undesirable noise. In-phase results give information about the real component and the quadrature results the imaginary component. [4-6].

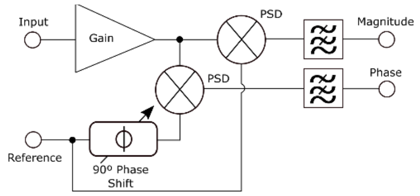

Fig. 1 - Classical LIA block diagram.

There are analog and digital versions of LIA available nowadays. Most digital designs use high resolution and high speed ADCs to capture the input signal and the reference signals are digitally created. Although LIAs have, in average, better performance than standard amplifiers under a noisy environment [7], those features make this approach costly.

This paper describes the implementation of a low cost LIA using a general purpose microcontroller, running a fast algorithm, connected to a computer for data visualization. In order to overcome the sampling rate limitation, the Nyquist condition is adopted by taking only two samples per period of the reference signal.

II. METHODOLOGY

As shown in Fig. 2, the in-phase result is obtained by sampling the amplitude of the input signal at phases 90º and 270º and computing its difference. The quadrature signal, in turn, is obtained by sampling the input signal at phases 0º and 180º and again computing its difference.

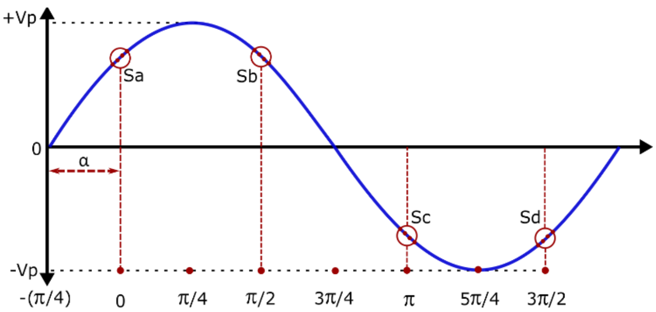

Fig. 2 - Sampling example for the proposed LIA.

Mathematically, the traditional [5] and the proposed PSD outputs for a generic sinusoidal function as reference are shown in Table 1.

Table 1 – Comparison between traditional and proposed approaches to the LIA.

LIA approach	Traditional	Proposed
In-Phase	$V = \frac{Vp}{2}\cos(\theta)$	$V = 2Vp\cos(\theta)$
Quadrature	$V = \frac{Vp}{2}\cos(\theta - \frac{\pi}{2})$	$V = 2Vp\cos(\theta - \frac{\pi}{2})$
Max. Output Voltage	$V = \frac{Vp}{2}$	$V = 2Vp$
Sampling Frequency	$10.f_{nf}$	$2.f_{nf}$
Mathematical Operation	Multiplication	Subtraction

A. Hardware

In order to achieve the objectives of this work, simulations were prepared with the goal of finding suitable components. Based on this, MSP430G2553 was the low cost and low power microcontroller chosen, along with other analog components.

The LIA proposed consists of a microcontroller and an analog band passs filter.

The microcontroller has an ADC of 10 bits but maximum operation speed, which involves sampling and processing, is limited. Since the system operates at the Nyquist condition the signal frequency is higher than a conventional digital LIA method where signal frequency needs to be much smaller than sampling frequency. Fig. 3 presents the microcontroller development board and its diagrams inside the dashed box, and the analog circuitry outside.

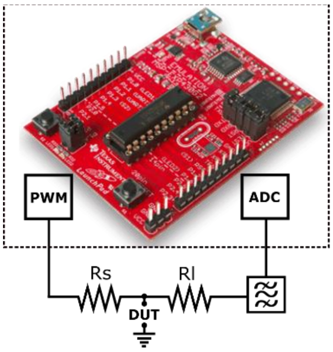

Fig. 3 - System diagram.

A PWM generates the reference frequency through a squared wave used to modulate the input signal amplitude. Then, the ADC capture samples of the input signal synchronously to the PWM's frequency. In order to take only the fundamental frequency of the square PWM wave, a second order band pass filter was designed before the ADC. The results are processed and sent to a computer via Universal Asynchronous Receiver-Transmitter (UART).

For the filter design, the center frequency chosen was 408Hz with a quality factor of 5. The resulting circuit is shown in Fig. 4 and its results simulation on Fig. 5.

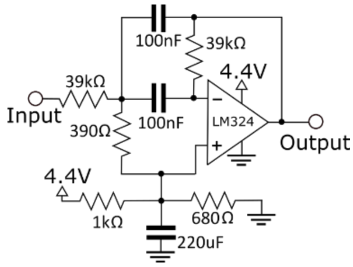

Fig. 4 – Band-pass filter design.

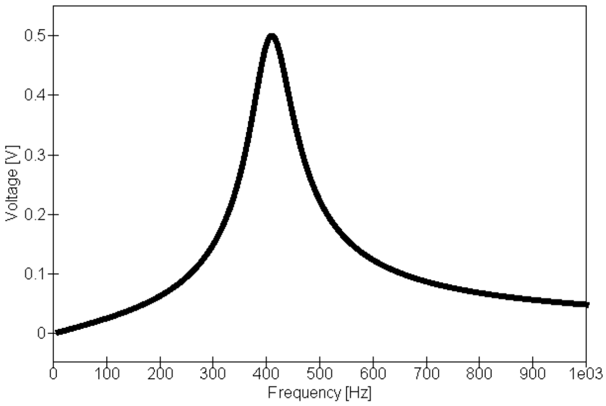

Fig. 5 - Frequency response to the second order band pass filter designed.

The main goal of the proposed LIA is to obtain the impedance of a DUT. In the excitation stage, the PWM signal is applied to the DUT through a known resistance Rs, responsible for limiting the current provided by the microcontroller. The other resistance Rl is a fixed, greater than Rs and represents the filter's input resistance. The DUT is placed between these two resistances and the ground.

The circuit measures the voltage Vx through the unknown impedance Zx (DUT). The proposed LIA has two outputs (one in-phase and another in-quadrature) allowing the calculation of the imaginary and real components of Vx, and the relative properties of reactive elements. Before measuring impedance, a calibration routine must be called to obtain short-circuit and open circuit voltages from the circuits shown in Fig. 6A and 6B, respectively. The resulting values are stored and used later to calculate the impedance.

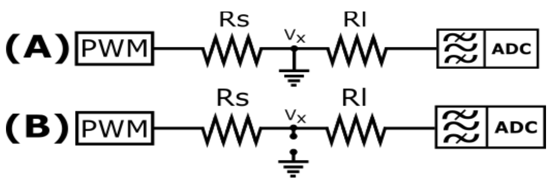

Fig. 6 - Calibration proceedings. (A) Short-circuit. (B) Open circuit.

Then, the unknown impedance is connected and V_X is measured. From basic circuit analysis and with use of previous calibrations, the unknown impedance can be calculated as shown below:

$$Z_x = \frac{R_l.R_s(V_{Rx} - V_{Rx} = 0)}{R_l + R_s(V_{Rx=\infty} - V_{Rx})}$$

Where R_l, R_s, V_{Rx}, $V_{Rx=0}$, $V_{Rx=\infty}$ are, respectively: Filter Input Impedance, source impedance [Ω], Voltage on the unknown impedance [V], short-circuit calibration voltage [V] and open-circuit calibration voltage [V] [4]. All the calculations are done considering complex numbers theory.

		Manufacturer Especification	LIA	LCR Meter Agilent 4263B	RE (%)
Inductor (mH)		2,60	2,78	2,68	3,96
		4,00	4,63	4,23	9,32
		16,00	18,38	16,32	12,63
Resistor (Ω)		15,00	14,23	14,87	4,30
		82,00	82,35	80,14	2,76
		180,00	195,28	179,5	8,79
Capacitor (nF)		13,74	15,12	13,45	12,43
		22,00	23,61	21,98	7,43
		27,48	28,7	27,01	6,26

B. Algorithm and Programming

The firmware was programmed in C on IAR Embedded Workbench Software.

The first step of the algorithm is to setup all peripherals the lock-in needed. MSP430 was setup with a 12MHz Main Clock Frequency. This is also used as clock source to the PWM in order to obtain a 408Hz frequency. In addition, the timer's interruption was configured to trigger on every PWM's fall edge. A HID (Human Interface Device) is configured, using UART communication between the microcontroller and USB serial port. After all setup subroutines are completed, the lock-in requires two calibrations routines. This can be triggered by using a push button.

During both open and short circuit calibrations, the interruption subroutine takes four samples, 90° phase shifted between each other. In order to increase the acquisition signal to noise ratio (SNR), the average of 64 samples are taken. The low pass LIA filter is digitally implemented through an exponentially weighted average filter (EWMA) with an alpha coefficient of 0,98. Giving a sampling frequency of 820Hz (Nyquist condition), the cut-off frequency of this filter is approximately 6.4Hz. In order to use less instructions and integer variables bit shift operations instead of multiplication and division. Once the calibration subroutine is finished, the lock-in starts to measure the desired impedance and sends the result through the serial port communication. The connected computer receives and displays the result of impedance module and phase for the DUT.

At a particular point of the development, it was noticed that the digital controlled oscillator (DCO) introduced error to the measurements due to spread spectrum. In order to solve the issue, an external crystal, already available in the LaunchPad, was connected to its specific microcontroller pin and configured in the clock sub routine.

III. Results and Discussion

In order to verify the range and accuracy of the LIA, measurements of discrete components were conducted and the results compared with the LCR Meter Agilent 4263B. Table 2 shows their performance based on impedance readings and the Relative Error (RE) regarding the LIA relative to the LCR measurements.

Table 2 – Inductance, resistance and capacitance measurements calculated from impedance measurements done by the LIA compared to those of the LCR.

It was possible to verify that the obtained relative error for discrete components allows reliable impedance measurements on values below the 10% error mark. Beyond that mark, the relative error was too expressive to ignore.

This phenomenon occurs due to hardware and scale limitations. The resistance R_s used before the DUT determines the sensitivity of the system and, consequently, the range of measurements to be made under an acceptable relative error margin.

The Mean Squared Error (MSE) for all resistances under the 180Ω mark and for each measuring was calculated. The proposed LIA presented an MSE of 1.44. The LCR Meter MSE was 0.78, which makes this LIA a good low cost solution in the range considered.

Expecting to represent practical applications such as passive sensors behavior and unknown impedances, RC, RL and LCR arrangements were analyzed. The results and each comparison for the impedance were depicted in tables 3, 4 and 5 for RC, RL and LCR circuits, respectively taking into consideration the RE.

Table 3 - Impedance measurement results for RC circuits.

LIA		LCR Meter Agilent		RE	
Magnitude (Ω)	Phase (°)	Magnitude (Ω)	Phase (°)	Magnitude (%)	Phase (%)
Series RC Circuit (R=15Ω C=13nF)					
$23{,}66.10^3$	-85,04	$98{,}68.10^3$	-90	76,01	7,13
Series RC Circuit (R=15Ω C=22nF)					
$15{,}52.10^3$	-85,04	$60{,}35.10^3$	-90	74,28	5,51
Parallel RC Circuit (R=15Ω C=13nF)					
14,32	-0,76	14,84	-0,55	3,54	38,18
Parallel RC Circuit (R=15Ω C=22nF)					
14,33	-0,39	14,71	-0,37	2,58	5,40

Table 4 - Impedance measurement results for RL circuits.

LIA		LCR Meter Agilent		RE	
Magnitude (Ω)	Phase (°)	Magnitude (Ω)	Phase (°)	Magnitude (%)	Phase (%)
Series RL Circuit (R=15Ω L=21mH)					
43,62	62,18	23,53	42,83	85,38	45,18
Series RL Circuit (R=15Ω L=2,5mH)					
16,19	23,56	15,463	7,13	4,70	230,43
Parallel RL Circuit (R=15Ω L=21mH)					
13,4	18,69	11,718	42,61	14,35	56,14

Parallel RL Circuit (R=15Ω L=2,5mH)					
5,38	60,44	2,3458	50,41	129,35	19,90

The high RE presented on table 4 was expected, since the input impedance R_s and input frequency were designed to measure higher values of inductance in series RL circuits. It was possible to verify that the obtained relative error for discrete components allows reliable impedance measurements on values below the 10% error mark. Beyond that mark, the relative error was too expressive to ignore.

Table 5 - Impedance and capacitance measurement results for capacitances values presented by all tested devices.

LIA		LCR Meter Agilent		RE	
Magnitude (Ω)	Phase (°)	Magnitude (Ω)	Phase (°)	Magnitude (%)	Phase (%)
Series LCR Circuit (L=2,5mH C=13nF R=15Ω)					
$23{,}41.10^3$	-84,58	99040	-89,92	76,35	5,94
Parallel LCR Circuit (L=2,5mH C=13nF R=15Ω)					
5,38	62,65	1,96	65,73	174,41	4,69

IV. CONCLUSION

From the results presented in this work, it was possible to validate the methodology proposed with accuracy similar to commercial devices for discrete components and specific arrangements. Some tested circuits showed high RE, which is consequence of a low scale parameter chosen for low impedance measurements and are influenced by frequency.

REFERENCES

[1] A. Restelli, R. Abbiati, and A. Geraci. **Digital field programmable gate array-based lock-in amplifier for high-performance photon counting applications.** Review of Scientific Instruments. September, 2005. DOI: https://doi.org/10.1063/1.2008991.

[2] Lars E. Bengtsson. **A microcontroller-based lock-in amplifier for sub-milliohm resistance measurements.** Review of Scientific Instruments. July, 2012. DOI: https://doi.org/10.1063/1.4731683.

[3] Gang Li (李刚), Shengzhao Zhang (张盛昭), Mei Zhou (周梅), Yongcheng Li (李永城), and Ling Lin (林凌). **A method to remove odd harmonic interferences in square wave reference digital lock-in amplifier**. Review of Scientific Instruments. February, 2013. DOI: ttps://doi.org/10.1063/1.4792596.

[4] NARDI, Maurício. **Analisador não invasivo da concentração de bilirrubina.** Federal University of Parana. Curitiba, 2017.

[5] NUNES, Rafael Astuto Arouche. **Desenvolvimento e aplicação o de um amplificador lock-in baseado em dsp.** Federal University of Rio de Janeiro, RJ, Brazil. August, 2009.

[6] Paul A. Remillard, Littleton, Mass.; Michael C. Amorelli, Danville, N.H. (1993). *U.S. Patent No. 5,210,484*. Washington, DC: U.S. Patent and Trademark Office.

[7] E. H. Fisher. **The Evolution of the modern Lock-in Amplifier, DL Instruments Technical Notes IAN35.** 2003. Available at: http://www.dlinstruments.com/ technotes/index.html